Dr. Ash

MARS METHANE ENGINE

Senior Design Project
MAE 434
Final Report

*III-37-
47 P*

April 21, 1994

Team Members:

Hung Bui

Chris Coletta
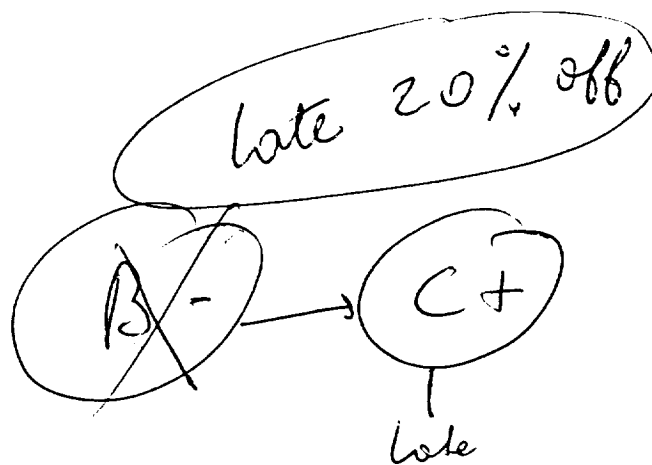
Alain DeBois

MARS METHANE ENGINE

Senior Design Project
MAE 434
Final Report

April 21, 1994

Team Members:

Hung Bui

Chris Coletta

Alain DeBois

Table of Contents

Abstract

The feasibility of an internal combustion engine operating on a mixture of methane, carbon dioxide, and oxygen has been verified by previous design groups for the Mars Methane Engine Project. Preliminary stoichiometric calculations examined the theoretical fuel-air ratios needed for the combustion of methane. Installation of a computer data acquisition system along with various ancillary components will enable the performance of the engine, running on the described methane mixture, to be optimized with respect to minimizing excess fuel. Theoretical calculations for stoichiometric combustion of methane-oxygen-carbon dioxide mixtures yielded a ratio of 1 : 2 : 4.79 for a methane-oxygen-carbon dioxide mixture. Empirical data shows the values to be closer to 1 : 2.33 : 3.69 for optimum operation.

1. Introduction:

The exploration of space, and specifically the surface of the planet Mars, presents many technical challenges. One specific challenge is operating an internal combustion engine on the Martian surface. One approach is to use the Martian atmosphere for the needed fuel, oxidizer, and diluent.

The Martian atmosphere consists of 95% carbon dioxide (CO_2), and water (H_2O) is believed to be plentiful from the ice deposits, therefore CO_2 and H_2O can be synthesized to produce methane (CH_4). Oxygen (O_2) can be used as an oxidizer and can be extracted by the thermal decomposition of CO_2 through a solid electrolyte process. Finally, CO_2 can be used as a diluent to the fuel and oxidizer in order to control combustion temperatures and minimize methane-oxygen consumption.

The goal of operating an internal combustion engine on methane, CO_2, and O_2 motivates the testing and analysis of the Honda GX120 4hp engine under laboratory conditions. Before CH_4, CO_2, and O_2 operation can be studied and optimized, certain objectives must be met. Since this is a continuing project that has been worked on by previous senior design teams, prior work must be reviewed and the hardware gathered to support further study. The project setup, including the data acquisition system, dynamometer, flow meters, engine, incremental encoder, and instrumentation must be groomed and brought back to specifications. Stoichiometric calculations must be made for operation with methane using air, as well as a CO_2 and O_2, as a diluent and oxidizer.

1

After the objectives are met, the goal of the engine operation and performance testing using methane, CO_2, and O_2 can be realized. Furthermore, operating data can be gathered for comparison and analysis.
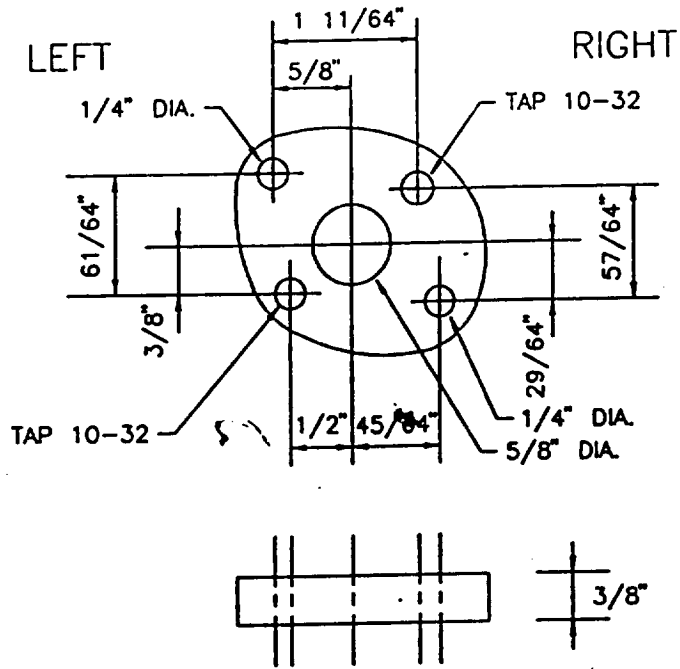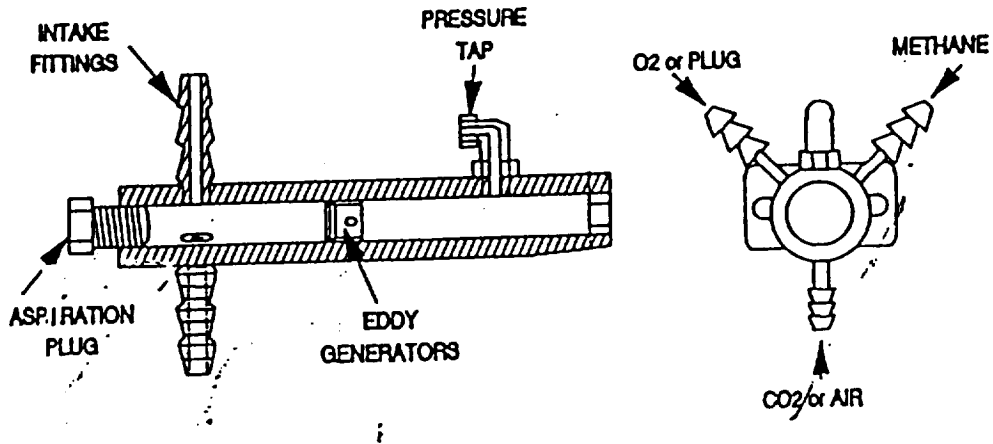
2. Background:

Funded by the NASA/USRA University Advanced Design Program, the Mars methane engine project has steadily progressed from a conceptual design to an actual functional apparatus. Currently three design teams have contributed to the project's mission objectives. The first design team, whose members were: Kieth Davis, Michael Uenking, and Wesely Wissinton [Wigginton], will hence forth be referenced in this report as the "Davis Team." The second team, of whom Scott Hoover, Stephen Lauer, Lori Lawrence, Chistos Paparistodemou, and Douglas Taylor were members, will likewise be referenced as the "Hoover Team."

At the project inception, the Davis Team had considerable difficulty adapting various internal combustion engine hardware for methane operation. This was realized when a stainless steel cylinder, used to replace the original fractured glass [cylinder] of the Megatech lab engine, still experienced difficulties.

However, great progress was achieved when the Hoover Team purchased a Honda GX120 4hp IC engine and its ancillary components. Construction of a "carburetor" has allowed the Honda engine to operate with either a gasoline/air mixture or a methane/CO_2/O_2 mixture (Please see Appendix A for Project Set-up). Figure 1 shows the current design of the adaptive carburetor design for methane use. Construction of the working prototype was performed by the Davis Team and was subsequently modified by the Hoover Team in the form of an adaptor also shown in Figure 1. Illustrations in Figure 1 were [was] taken from the Hoover Team's final report.

3

INTAKE FITTINGS

PRESSURE TAP

O2 or PLUG

METHANE

ASP.IRATION PLUG

EDDY GENERATORS

CO2/or AIR

LEFT

RIGHT

1 11/64"

5/8"

1/4" DIA.

TAP 10-32

61/64"

57/64"

3/8"

29/64"

TAP 10-32

1/2" 45/64"

1/4" DIA.

5/8" DIA.

3/8"

CARBURETOR ADAPTOR

Figure 1: Modified Carburetor and its Adaptor

4

Through their efforts, the Hoover Team was able to obtain data from the combustion of methane in air (base case) and the combustion of a methane/CO_2/O_2 mixture. Obtaining performance data for the test case was significant since this allowed the team to achieve its design objectives. Although the Hoover Team obtained data for their test case, their results were ~~skewed~~ in error due to dynamometer anomalies explained later in this report.

3. Progress and Results:

It was the intent of the current design team to thoroughly review all prior engine work completed by previous teams during the first phase of the project (please see Gantt Chart in Appendix B). Checking and verifying the previous team's preliminary calculations for required air-to-fuel ratios of methane and air proved to be a rather laborious yet necessary undertaking. From this analysis, we immediately began testing the engine using the standard gasoline-air mixture. We chose to bypass methane-air testing, since this process was thoroughly investigated by the Hoover Team, and proceed directly to methane-oxygen-carbon dioxide operation. It was planned use results from the chemical analysis of the exhaust gas sample from the methane-air operation to verify stoichiometric calculations, but we have discovered that this was unnecessary. Methane-air operation was used to verify that the engine can successfully run on methane. Whether or not the engine burns the correct stoichiometric ratio of fuel to air is unimportant. What was important was that it can burn methane at all. Now that we know that the engine can indeed run on methane, we can proceed to methane, CO_2 and O_2 operation.

3.1 Gasoline/Air--Methane/Air Operation:

Since most of the engine apparatus was installed by the previous team, a goal of this Team was to ensure that the components were still operational as intended. By operating the engine on a gasoline and air

mixture, we can test the functionality of the engine with respect to the previous team's results.

During our testing, we have found that for gasoline and air operation, the engine constantly operated above the testing limits of the Megatech dynamometer. Power and torque versus revolutions per minute curves generated by the previous design team had not shown the Honda engine's actual maximum power nor torque capabilities, in accordance with Honda's specifications. This can be a major obstacle since accurate curves relating to engine performance are required for effective comparison of engine efficiencies between gasoline/air and methane/air operation.

Performance Curves for Honda GX120
Unleaded Gasoline (Full Throttle)
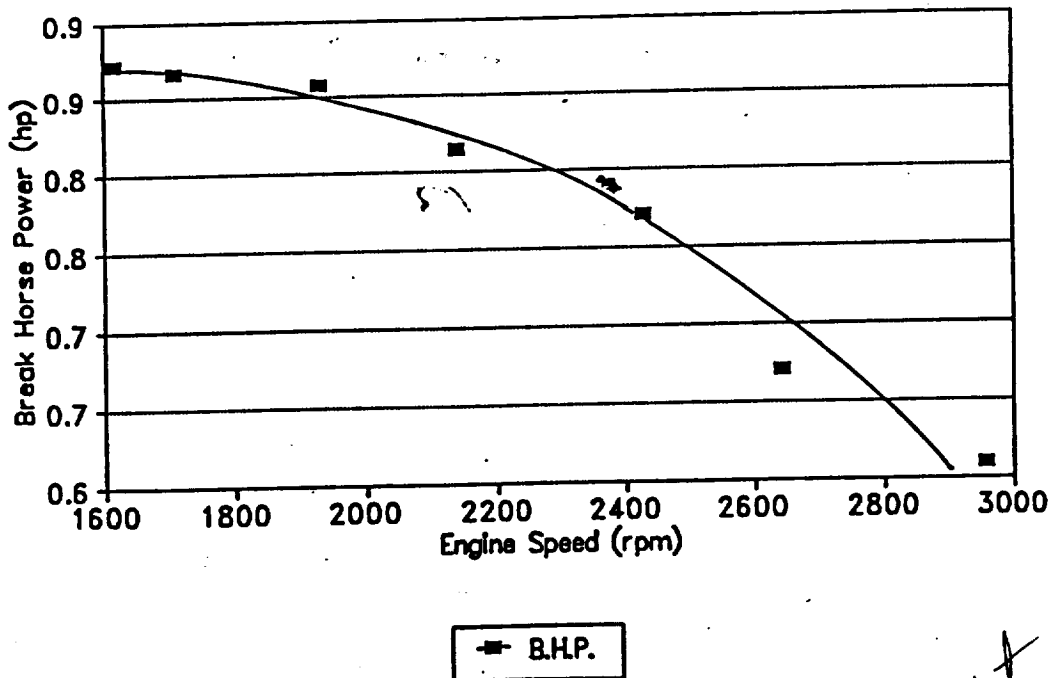
Figure 2: Power versus RPM

Performance Curves for Honda GX120
Unleaded Gasoline (Full Throttle)
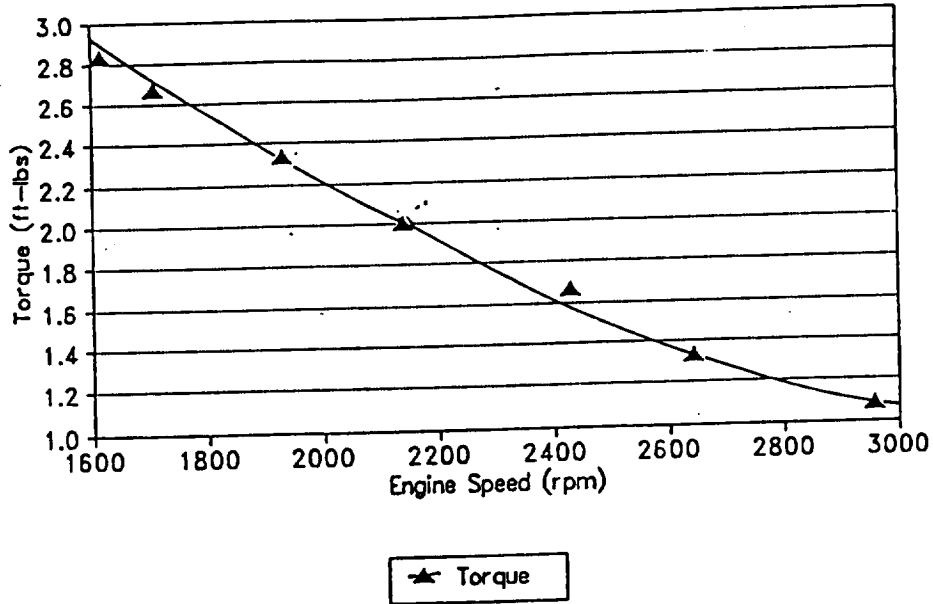
Figure 3: Torque versus RPM
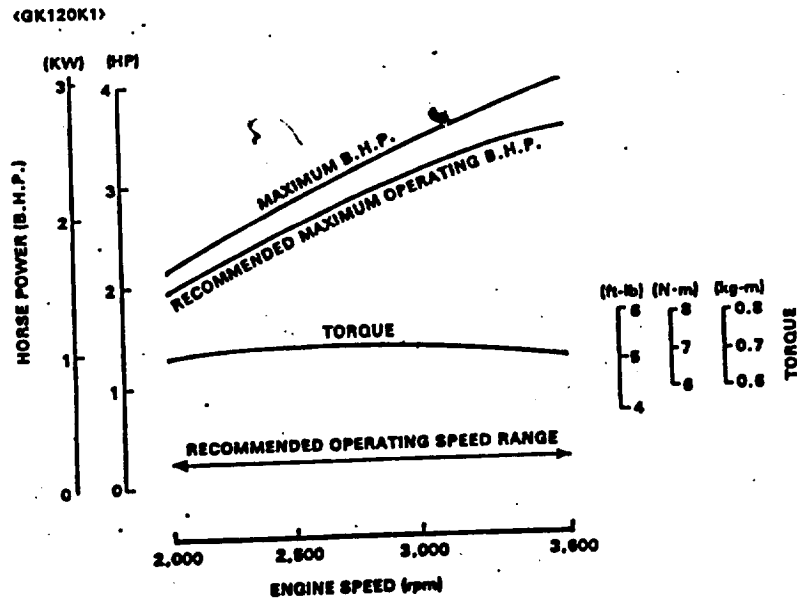
Figure 4: Honda GX120 Power and Torque Specifications

8

Both Figures 2 and 3, generated by the Hoover Team, from their data on gas operation in their final report, show curves that are inconsistent with Honda's curves (Figure 4). However, during our review of their data, we were able to operate the engine on gasoline and duplicate their results. *(Whose results?)* From our results, we were now in a position to verify the inconsistencies in their data.

The dynamometer was limited to a maximum of 60 in-lb of torque while the engine, operating at peak power, produced nearly 66 in-lb of torque. Looking at Figure 4 taken from the Honda owner's manual, one can observe that the entire torque range of the engine lies above the dynamometer's 60 in-lb limits.

To acquire the Hoover Team's data for gasoline, we arbitrarily selected a reference torque value below the maximum torque (i.e. 50 in-lb at 2800 rpm) then varied the load while keeping a constant throttle. Figure 5 shows the data we generated from this experiment. Obviously, this procedure generates data for either gas or methane operation, but the data collected would not be a true representation of the engine's capability at maximum power throughout its rpm range. *(why?)*

RPM	Torque (in-lbs)
3600	16
3500	17
3400	20
3300	21
3200	22
3100	28
3000	32
2900	41
2800	50
2700	54

Figure 5: Constant Throttle/Varying Load For Gasoline

3.2 Data Acquisition:

The Data acquisition system is composed of an IBM compatible computer running on an Intel 80286 microprocessor with an 80287 math coproccessor. Data Translation provided the DT2811 data acquisition board necessary for taken engine data measurements in real time. The pressure transducer, whose output is changes in microvoltages, is fed into a charged amplifier for signal amplification. A thermocouple, attached to the exhaust manifold of the engine feeds changes in temperature to the system. Temperature data can be used as a base to sample changes to the actual combustion chamber temperatures, although it must be noted that it is not a true record of the actual combustion temperature. However, for our purposes, rising temperature was used to verify that combustion had indeed ocurred. The incremental encoder, although useful, was not used by the

current team. Its output signals were base on changes in current values over time. The DT2811 accepts input signals based on changes in voltages over time, hence making it incompatible with the encoder, The Hoover Team bypassed this problem by constructing a circuit, using a 16-pin CMOS chip which was not referenced in their final report. Their circuit was supposed to convert the current based signal to a voltage based signal compatible with the DT2811. Since they also failed to correctly program the encoder, we could not assume their circuit was operational.

An operational encoder would enable the data acquisition system (programmed in FORTRAN), to read instantaneous volume displacements as function of crank angle with respect to time (which, in turn, is a function of rpm). This data, coupled with the pressure transducer data over the same period of time, would allow the construction of a power indicator diagram (pressure versus volume). From the areas enclosed by the curves, we can use numerical methods to extract work. From this data we can make direct comparisons of efficiency and power capacities between methane-air, methane-oxygen-carbon dioxide, and gasoline-air.

3.3 Methane-CO$_2$-O$_2$ Operation:

In order to operate the engine using the gas bottles in a manner such that safety was the major emphasis, a thorough investigation into safety analysis was performed. From our analysis, we found that moving the entire apparatus nearer to available power sources and cooling water supplies greatly reduced the likelihood of potential hazards. Securing the gas bottles and flow meter component boards also reduced the risk of

accidents. We also developed a procedure for methane operation that would ensure that various equipment and appropriate valves and switches are in their proper positions. The procedure to start the engine for methane operation is as follows:

Start-up procedure for Honda GX120 4Hp IC engine on methane, CO_2 and O_2:

1. Supply cooling water for pressure transducer.
2. Close the flow meters from the methane, CO_2 and O_2 gas bottles.
3. Establish a back pressure of 100 kPa on the methane, CO_2 and O_2 gas bottles.
4. Connect a 12 volt battery to the DC input terminals on the dynamometer and turn on AC power supply.
5. Turn Honda engine switch to 'ON' position.
6. Set dynamometer to 'START' operational mode, 'CW Field Mode,' and 'HIGH Load Range.'
7. Increase Field Load potentiometer on dynamometer until engine shaft begins to rotate. *(after, reading the data on the flow)*
8. Adjust methane, CO_2 and O_2 flow meters to obtain combustion while maintaining a ratio of 1 : 2 : 4.7 as predicted by the stoichiometric combustion equation.
9. When combustion occurs, set dynamometer Operational Mode to desired field load.
10. Adjust gas flowrates and field load for optimum rpm
11. Run data acquisition program for exhaust temperature and cylinder pressure.
12. To secure engine and dynamometer:
    Secure methane, CO_2 and O_2 flow meters;

Close valves!

Select engine switch to 'OFF'

Secure gas bottles

Secure AC Power to dynamometer

Secure Cooling water to pressure transducer

In step number 8, the ratio of 1 : 2 : 4.7 was arrived at on a theoretical basis from a stoichiometric calculation (please see Appendix C). Starting with this ratio, we were able to get the engine to fire, however the engine seemed to be "choking" in its operation. Reactively, we immediately increased methane flow to a level where the engine ran without choking. Eventually we arrived at an empirical ratio of 1 : 2.33 : 3.69 for most of the rpm range. This result would seem to indicate that the engine was running on excess O_2. This is good since this would tend to minimize the amount of fuel we would need to use per mole of O_2. No !!

However, we were concerned that the diluent level was much lower than predicted. The next logical step would be to determine what the impact of varying CO_2 levels would have on both engine operation and stoichiometric ratios. From the graph on Figure 6, we can see that changes in CO_2 level why? affects engine running temperature. Also in Appendix D the data shows that the engine quickly reaches operating temperature and fluctuates about this point through out its operation. The pressure read from the pressure transducer fluctuates as it did during gas operation.

CO2 FLOWRATE VERSUS EXHAUST GAS TEMPERATURE
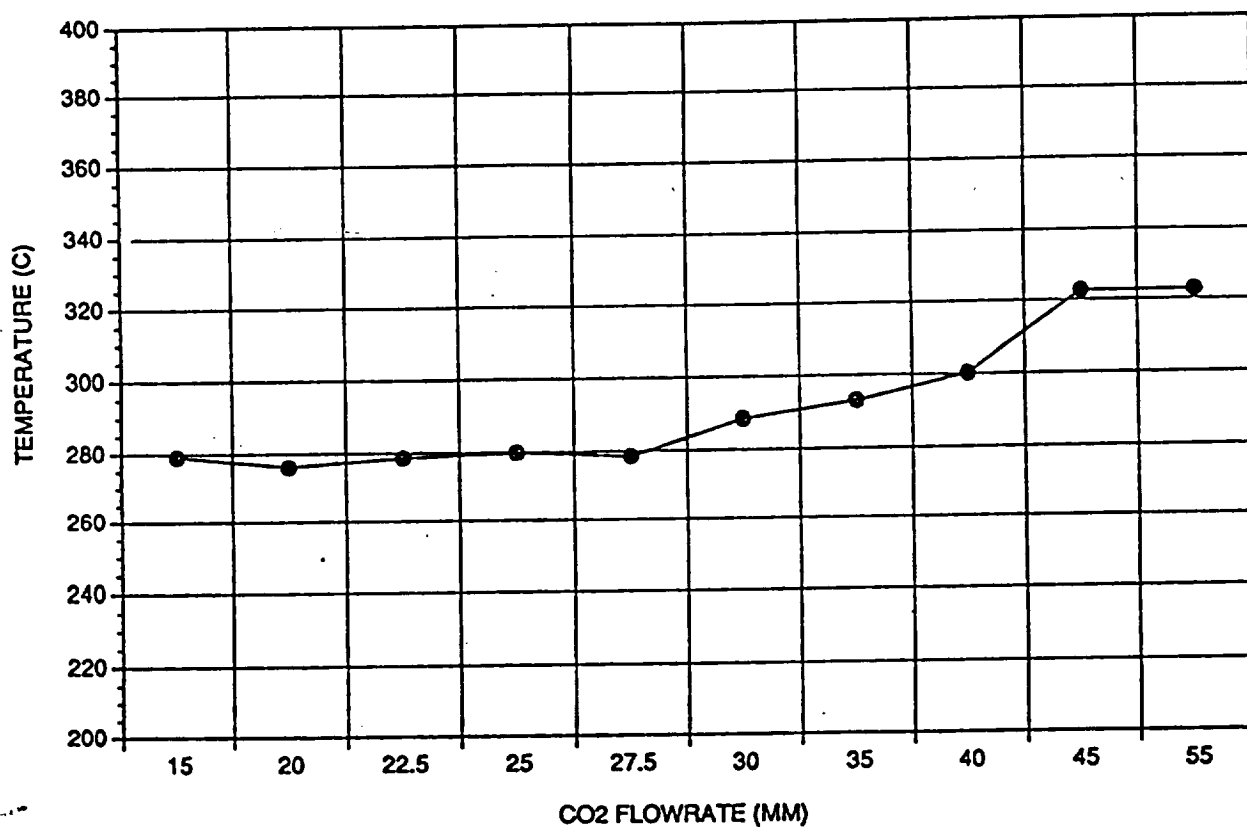
Figure 6: CO_2 Flowrate vs. Exhaust Gas Temp.

4. Future Goals of the Project:

What about the encoder?

Future work on the Mars methane engine project will concentrate upon expanding the database of engine performance in order to maximize efficiency at various power ratings. All engine modifications are complete and the apparatus is functioning properly. With exception to the incremental encoder, the data acquisition system is operative.

An objective for the next design team would be to refine the incremental encoder program to give instantaneous cylinder volume readings during engine operation. The encoder program is necessary for calculating the volume in the piston as a function of crank angle. The volume calculation is vital for establishing the pressure versus volume diagram (indicator diagram) necessary to analyze the performance of an internal combustion engine. Once the indicator diagram is generated, the work resulting form the bottle supply pressure can be separated from the actual work resulting from the fuel combustion. Calibration curves for the flow meters must be acquired for more accurate combustion analysis. The flow meters currently measures in millimeter units. To effectively consider combustion analysis, actual volumetric flowrates must be known. This obstacle is currently bypassed by applying the ratios obtained from stoichiometric calculations to the flow meter.

A higher performance rated dynamometer should be acquired for future considerations of gas-air operating characteristics. In order to compare the performance of the Honda engine operating on methane versus methane operation, data must be collected for gas operation at all performance levels. The current dynamometer cannot handle the engine operating on gas at maximum power levels with blowing the reset-able fuse. Future design

15

teams may have access to a higher rated dynamometer that the MET
department is considering to purchase. *~is~ outboard*

Major challenges to this team arose from the lack of knowledge of
where various instrumentation and engine components were located.
Assorted manuals and documentation often necessary for calculations and
instrumented *~ation~* operation were haphazardly placed in unknown locations
throughout the building and testing area. The practice of accurate record
keeping and finding a centralized location for all relevant material
concerning the project followed by the current team and suggested for
subsequent design teams should keep the project's transition from team to
team more streamlined and efficient. *← Did you fix this?*

4.1 Possible Design Considerations:

Future design teams, once they have completely installed every
possible piece of equipment relating to data acquisition, can generate power
indicator diagrams for comparison purposes. However, it is the belief of the
current team that the testing limits of the Honda gasoline engine is being
rapidly approached. With reference to Dr. Ash's comments, the testing of
this engine has gone as far as it will go with an "off-the-shelf" gasoline
engine. To obtain more realistic data for methane operation, we need an
engine that is optimized for such operation. This optimization could entail
possible cylinder/valves redesign, lower temperature operation for less
thermal wear, and multiple spark plugs for more even and controlled flame
propagation during detonation. Operating the engine on a Diesel cycle would
provide some results, but at such high compression ratios required in a

Diesel cycle, maintenance would be at a premium. To achieve some of these design considerations, we need to examine the processes of an air standard Otto cycle and modify it for adaptive use on a "Martian standard" cycle.

In an air standard Otto cycle, thermal efficiency depends basically on the compression ratio (CR) and $K=C_p/C_v$ where C_p and C_v are heat capacities. The efficiency for the Otto cycle would simply be:

$$\eta_{eff} = 1 - \frac{1}{(CR)^{K-1}} \qquad \text{(Equation 1)}$$

From equation 1, we can see that by raising the compression ratio, we can increase the efficiency. Unfortunately, increasing compression ratio above a certain point becomes impractical since this places more stress on the cylinder assembly and may result in pre-detonation of the fuel-air mixture (knocking). On the surface of Mars, where ambient pressures are one-seventh of that on Earth, increasing CR may not be a good idea since engine repairs and frequent retuning would prove impractical and risky. Also power hungry blowers, turbochargers, intercoolers, etc. needed to operate such an engine at a high CR value would be heavy and cumbersome. A possible tradeoff would be to operate the engine on a Miller cycle.

The Miller cycle, while similar to the Otto cycle, would allow the engine to operate with less wear and tear. This cycle is not used in today's engine design because the ratio between design and production costs and minor increases in performance over the Otto cycle is not great. However, for a prototype methane engine requiring a minimum amount of repairs, this works just fine.

17

An engine designed to operate on an Otto cycle would ideally have an isentropic compression stage, a combustion/detonation stage, and an isentropic expansion/work stage. In the Miller cycle, an air-fuel mixture would be pumped into the cylinder rather than drawn in by the downward suction from the piston as in the Otto cycle. The only difference here would be that the intake valve(s) in the Miller cycle would not fully close until the piston is well into its compression stage from bottom dead center. The result is greater time for the piston/cylinder assembly to cool allowing cooler operating temperature, and a much reduced compression ratio. Combustion would still occur at top dead center as in the Otto cycle and the full expansion/work process would still take place. The final result: less wear and tear on the valve assemblies due to a lower compression ratio and less thermal wear and increased lubricating oil life due to minimum oil viscosity breakdown from a lower operating temperature.

This is a very of logic. strange turn How did you get from diesel to "Miller"?

Where are your results?

5. Conclusions:

Analysis of the Mars methane engine has given significant insight to the engine's power capabilities. Although a great amount of time was spent getting the data acquisition system functioning properly, significant data has been collected on the performance of the methane engine.

Stoichiometrically calculated flowrates were not satisfactory in actual testing because back pressures and the engine's optimization for gas operation was not taken in to consideration. Alternatively, good performance data was acquired as the levels of methane, oxygen, and carbon dioxide were varied for several runs. A throttling effect was observed as levels of methane were increased. Data was also collected holding methane and oxygen levels constant and varying the carbon dioxide levels. The flowrate of the diluent carbon dioxide had a direct correlation with the operating temperature of the engine. As the level of carbon dioxide increased, so did the running temperature of the engine. *why?*

Methane operation was successfully tested using the current dynamometer since the maximum load attained was only half the rated load of the dynamometer. The maximum load under gas operation was never achieved because of the dynamometer could not handle the load.

? Conversion of the Honda engine from gasoline to methane yielded successful performance data despite the fact that the engine was originally designed to operate on gasoline. Methane performance data may not seem to be impressive, but methane operation can be optimized to its full potential in an engine specifically designed and calibrated for methane operation. These results may be a cornerstone for the methane engine designed to operate on *?* Mars. *Where is the data?*

References

1. Campell, Ashley, S., *Thermodynamic Analysis of Combustion Engines*, Robert E. Kreiger Publishing Company, Malabar, Florida, 1986.

2. Ferguson, Colin R., *Internal Combustion Engines*, John Wiley and Sons., New York, 1986.

3. GX120K1 Owner's Manual, Honda Power Equipment, 1991 Honda Motor Co.

4. Jennings, Burgess H., Obert, Edward F., *Internal Combustion Engines, Analysis and Practice*, International Textbook Company, PA, 1944.

5. Lauer, Stephen, et al., *Mars Methane Engine, Senior Design Project*, April 23, 1993.

6. Mooney, David A., *Introduction to Thermodynamics and Heat Transfer*, Prentice -Hall, Inc. N.J., 1955.

7. Obert, Edward F., Gaggioli, Richard A., *Thermodynamics*, McGraw-Hill Book Company, New York, 1963.

8. Weston, Kenneth C., Energy Conversion, West Publishing Company, New York, 1992.

9. Wylen, Gordon J., Sonntag, Richard E., *Fundamentals of Classical Thermodynamics* 3rd Ed., John Wiley & Sons, New York, 1985.

Appendix A

FLOWMETER

TO
CARBURETOR

THERMOCOUPLE
(TO D/A SYS.)

PRESSURE TRANSDUCER
(TO D/A SYS.)

CARBURETOR

DATA
ACQUISITION
SYSTEM

EXHAUST GAS
SAMPLE CYLINDER

O_2

CO_2

CH_4

TO
DYNAMOMETER

12V.
BATTERY

+

−

PUMP

COOLING
SYSTEM FOR
PRESS. TRANS.

ENCODER   ENGINE   DYNAMOMETER

MOUNTING STAND
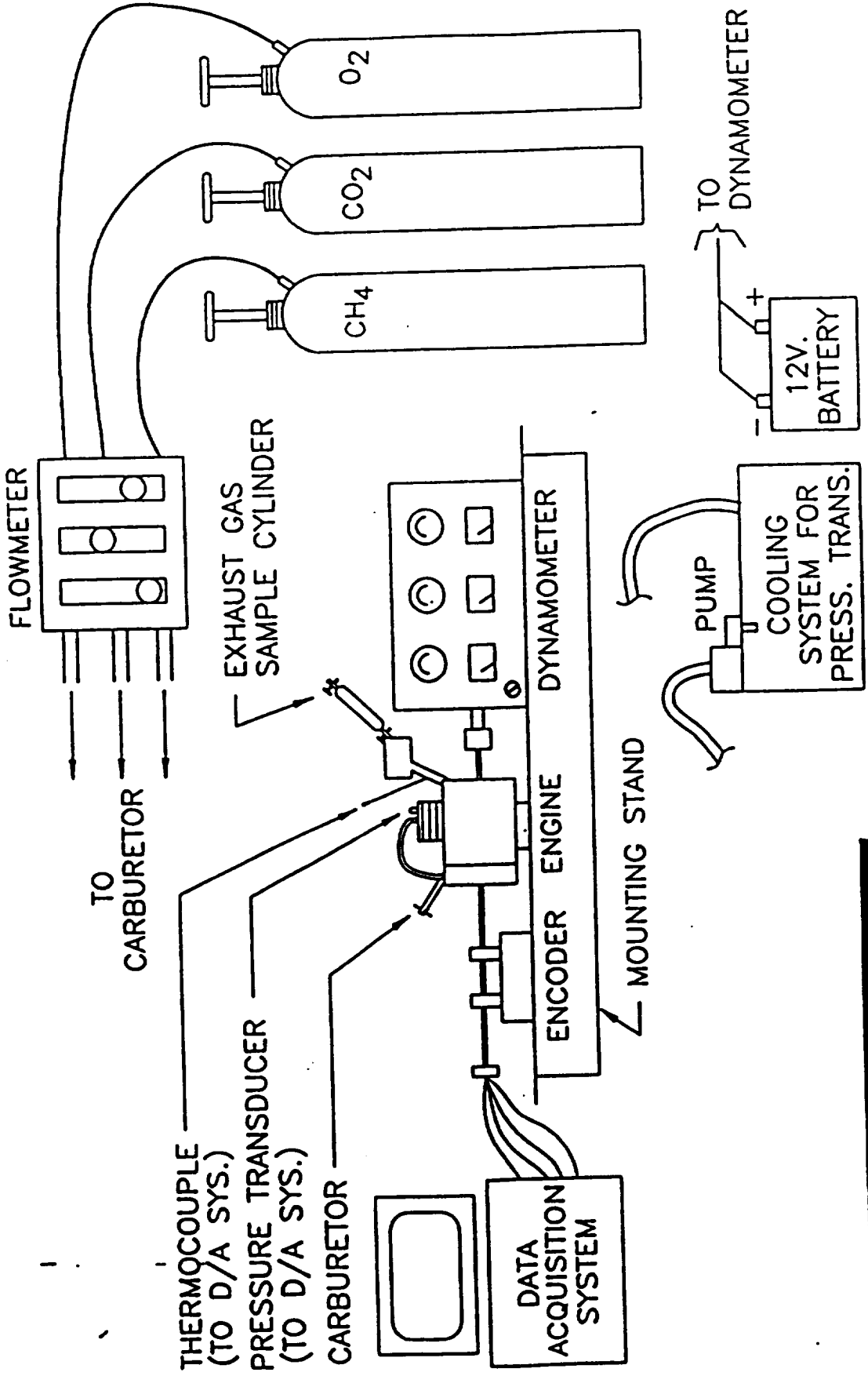
PROJECT SET−UP

MARS METHANE ENGINE
SENIOR DESIGN PROJECT MEM434

SHT.
1

Appendix B

MILESTONE CHART

Mars Methane Engine

4/21/94

Task Descriptions	Date	January	February	March	April
Review All Prior Work	A.S. 1/14/94 A.F. 2/11/94	████████			
Safety Review	A.S. 1/18/94 A.F. 2/11/94	██████			
Engine Set Up/Operational Learning	A.S. 1/24/94 A.F. 2/11/94	███			
Set Up Data Acq. System	A.S. 1/24/94 E.F. 4/9/94	██████████████████			
Study Exhaust Gas Analysis Procedures	A.S. 1/18/94 E.F. 3/8/94	█████████████			
Gasoline/Air Operation/Review	A.S. 1/24/94 E.F. 2/28/94	████████			
CH4/Air Operation/Review	A.S. 2/8/94 E.F. 3/8/94		██████		
CH4/CO2/O2 Operation/Review	A.S. 2/22/94 E.F. 4/9/94		███		
Perform Stoichiometric Calculations	A.S. 2/14/94 E.F. 3/8/94		█████		
Collect All Data For Comparison/Review	A.S. 3/8/94 E.F. 4/9/94			██████	
Final Technical Report/Presentation	A.S. 4/1/94 E.F. 4/19/94				███

A.S. - Actual Starting Date   E.F. - Estimated Completion Date   A.F. - Actual Completion Date

Appendix C

CALIBRATION OF PRESSURE TRANSDUCER

MANIPULATION OF CHARGE AMPLIFIER

$$S = \frac{\text{TRANS. SENS.} * P_{max} \text{ measurement} * V_{out} max (v)}{\text{RANGE} * V_{out} (V)}$$

where: (S) is the value in pC/bar
to be set at the potentiometer

V_{out} max = 5V

TRANS. SENS. (pC/bar)	10.98
pmax (bar)	15
Range (bar)	100

$$S = \frac{10.98 * 15 * 5}{100 \times 5} = 1.647$$

Note:

To give a specific output voltage of 5V for a specific input pressure, an "incorrect" transducer sensitivity value of 1.647 is set at the push button potentiometer on the charge amplifier.

STOICHIOMETRIC CALCULATIONS FOR METHANE (CH4) WITH 100% THEORETICAL AIR COMBUSTION EQUATION

Combustion Equation (AIR)

$$1 \; CH_4 + 2 \; O_2 + 7.52 \; N_2$$
$$\longrightarrow 1 \; CO_2 + 2 \; H_2O + 7.52 \; N_2$$

Combustion Equation (CO_2/O_2)

$$1 \; CH_4 + 2 \; O_2 + 4.79 \; CO_2$$
$$\longrightarrow (1 + 4.79) \; CO_2 + 2 \; H_2O$$
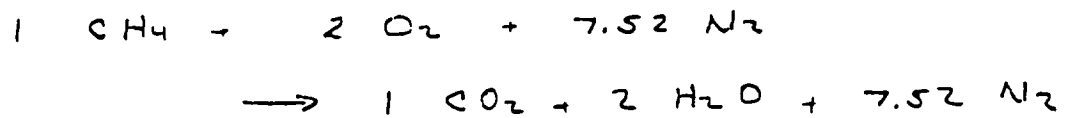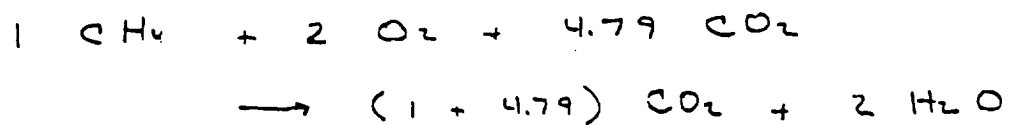
Substance	Molecular Symbol	Atomic Weight
Carbon	C	12
Hydrogen	H	1
Oxygen	O	16
Nitrogen	N	14

To compute the equivalent amount of CO_2 to be used in place of N_2:

$$7.52 \; N_2 = (7.52)(2)(14) = 210.56$$
$$X \; CO_2 = X (12 + 32) = 210.56$$
$$X = 4.79 \; kmoles \; of \; CO_2$$

- **AIR / FUEL RATIO**

$$\left.\frac{AIR}{FUEL}\right)_{mass} = \frac{2\ O_2 + 7.52\ N_2}{1\ CH_4}$$

$$= \frac{2\,(32) + 7.52\,(28)}{16}$$

$$= 17.16$$

- **$(CO_2 \text{ & } O_2)$ / FUEL RATIO**

$$\left.\frac{(CO_2 \text{ & } O_2)}{FUEL}\right)_{mass} = \frac{2\ O_2 + 4.79\ CO_2}{1\ CH_4}$$

$$= \frac{2\,(32) + 4.79\,(12+32)}{1\ CH_4}$$

$$= 17.17$$

Conclusion:

The air/fuel ratio is equivalent to the $(CO_2 \text{ & } O_2)$/fuel ratio and lends justification to the use of the combustion equation for 100% theoretical air for stoichoimetic calculations for CH_4 / CO_2 / O_2.

Appendix D

Gasoline/Air Operation

THERMOCOUPLE TYPE	CHANNEL	TEMPERATURE (C)
75	4	215.634600

Load setting = 3 Torque = 34 in-lb rpm = 3600

atm press = 762 mm Hg amb temp = 20 C

THE FREQUENCY OF THIS RUN IS:
1.000000

THE NUMBER OF COUNTS:
100

VOLTS	DEGREES C	TIME(SEC)	PRESSURE(PSIG)
-.634766E-01	215.635	1.0000	-9.33
.488281E-01	214.375	2.0000	7.18
-.732422E-01	214.423	3.0000	-10.76
.634766E-01	215.635	4.0000	9.33
.244141E-01	215.017	5.0000	3.59
.117188E+00	215.635	6.0000	17.22
-.537109E-01	215.682	7.0000	-7.89
-.512695E-01	215.682	8.0000	-7.53
-.488281E-01	215.635	9.0000	-7.18
.122070E+00	215.635	10.0000	17.94
.207520E+00	216.300	11.0000	30.50
-.268555E-01	216.252	12.0000	-3.95
-.561523E-01	215.635	13.0000	-8.25
-.439453E-01	216.847	14.0000	-6.46
-.195313E-01	216.847	15.0000	-2.87
.488281E-01	216.894	16.0000	7.18
.488281E-02	215.635	17.0000	.72
-.195313E-01	216.847	18.0000	-2.87
-.659180E-01	216.252	19.0000	-9.69
.141602E+00	215.682	20.0000	20.81
-.537109E-01	215.635	21.0000	-7.89
.178223E+00	216.252	22.0000	26.19
-.122070E-01	216.252	23.0000	-1.79
.117188E+00	216.847	24.0000	17.22
.114746E+00	216.799	25.0000	16.86
.903320E-01	217.464	26.0000	13.28
.310059E+00	216.252	27.0000	45.57
-.512695E-01	217.464	28.0000	-7.53
-.781250E-01	216.252	29.0000	-11.48
-.732422E-01	216.847	30.0000	-10.76
-.781250E-01	216.799	31.0000	-11.48

-.805664E-01	216.847	32.0000	-11.84
-.756836E-01	218.106	33.0000	-11.12
-.830078E-01	216.300	34.0000	-12.20
-.463867E-01	216.847	35.0000	-6.82
-.195313E-01	217.464	36.0000	-2.87
-.610352E-01	217.464	37.0000	-8.97
.239258E+00	216.847	38.0000	35.16
-.170898E-01	217.464	39.0000	-2.51
.192871E+00	217.512	40.0000	28.35
-.561523E-01	217.464	41.0000	-8.25
-.415039E-01	216.300	42.0000	-6.10
-.219727E-01	218.106	43.0000	-3.23
-.585938E-01	216.847	44.0000	-8.61
.256348E+00	217.512	45.0000	37.67
-.366211E-01	217.464	46.0000	-5.38
.170898E-01	216.847	47.0000	2.51
.148926E+00	216.847	48.0000	21.89
-.122070E-01	216.894	49.0000	-1.79
.244141E-02	218.058	50.0000	.36
-.415039E-01	218.058	51.0000	-6.10
.187988E+00	217.512	52.0000	27.63
.390625E-01	218.058	53.0000	5.74
-.830078E-01	218.058	54.0000	-12.20
-.537109E-01	218.058	55.0000	-7.89
.256348E+00	218.724	56.0000	37.67
.512695E-01	218.058	57.0000	7.53
-.585938E-01	218.724	58.0000	-8.61
.117188E+00	218.058	59.0000	17.22
-.561523E-01	219.294	60.0000	-8.25
-.634766E-01	218.058	61.0000	-9.33
-.488281E-01	218.676	62.0000	-7.18
-.952148E-01	218.058	63.0000	-13.99
-.683594E-01	218.058	64.0000	-10.05
-.927734E-01	218.011	65.0000	-13.63
-.708008E-01	219.294	66.0000	-10.41
-.781250E-01	218.106	67.0000	-11.48
-.117188E+00	217.464	68.0000	-17.22
-.119629E+00	218.724	69.0000	-17.58
-.112305E+00	219.294	70.0000	-16.51
-.104980E+00	218.676	71.0000	-15.43
.114746E+00	218.629	72.0000	16.86
-.124512E+00	218.676	73.0000	-18.30
-.134277E+00	219.294	74.0000	-19.73
-.634766E-01	218.724	75.0000	-9.33
.676270E+00	217.464	76.0000	99.39
.488281E+00	219.247	77.0000	71.76
.798340E+00	219.247	78.0000	117.33
.244141E-01	218.676	79.0000	3.59
.725098E+00	218.106	80.0000	106.57

-.732422E-01	219.294	81.0000	-10.76
.505371E+00	219.342	82.0000	74.27
-.341797E-01	219.294	83.0000	-5.02
-.927734E-01	219.888	84.0000	-13.63
-.119629E+00	218.058	85.0000	-17.58
.927734E-01	219.342	86.0000	13.63
-.119629E+00	220.506	87.0000	-17.58
.375977E+00	219.888	88.0000	55.26
-.878906E-01	219.841	89.0000	-12.92
-.134277E+00	220.506	90.0000	-19.73
-.144043E+00	221.148	91.0000	-21.17
-.129395E+00	219.888	92.0000	-19.02
-.366211E-01	218.724	93.0000	-5.38
-.903320E-01	221.148	94.0000	-13.28
-.139160E+00	219.888	95.0000	-20.45
-.122070E-01	220.554	96.0000	-1.79
-.610352E-01	221.148	97.0000	-8.97
-.136719E+00	220.506	98.0000	-20.09
-.561523E-01	220.506	99.0000	-8.25
.290527E+00	219.936	100.0000	42.70

Methane/oxygen/Carbon Dioxide

THERMOCOUPLE TYPE	CHANNEL	TEMPERATURE (C)
75	4	264.701400

THE FREQUENCY OF THIS RUN IS:
1.000000

THE NUMBER OF COUNTS:
200

VOLTS	DIG. VAL	DEG C	TIME(SEC)	PRESSURE(PSIG)
-.012207	2043	265.301	1.0000	-1.79
-.014648	2042	264.701	2.0000	-2.15
-.046387	2029	264.124	3.0000	-6.82
-.034180	2034	264.748	4.0000	-5.02
-.051270	2027	264.701	5.0000	-7.53
-.053711	2026	264.748	6.0000	-7.89
-.061035	2023	265.301	7.0000	-8.97
-.061035	2023	265.348	8.0000	-8.97
-.058594	2024	265.901	9.0000	-8.61
-.061035	2023	265.509	10.0000	-8.97
-.063477	2022	265.994	11.0000	-9.33
-.063477	2022	264.124	12.0000	-9.33
-.058594	2024	265.901	13.0000	-8.61
-.065918	2021	265.348	14.0000	-9.69
-.061035	2023	265.994	15.0000	-8.97
-.063477	2022	265.994	16.0000	-9.33
-.065918	2021	265.948	17.0000	-9.69
-.063477	2022	265.901	18.0000	-9.33
-.061035	2023	266.478	19.0000	-8.97
-.063477	2022	266.525	20.0000	-9.33
-.061035	2023	265.394	21.0000	-8.97
-.065918	2021	265.348	22.0000	-9.69
-.065918	2021	265.855	23.0000	-9.69
-.063477	2022	265.855	24.0000	-9.33
-.061035	2023	265.948	25.0000	-8.97
-.058594	2024	265.855	26.0000	-8.61
-.058594	2024	265.901	27.0000	-8.61
-.061035	2023	267.079	28.0000	-8.97
-.068359	2020	266.478	29.0000	-10.05
-.070801	2019	266.571	30.0000	-10.41
-.078125	2016	265.855	31.0000	-11.48
-.075684	2017	265.948	32.0000	-11.12
-.065918	2021	266.525	33.0000	-9.69
-.043945	2030	266.571	34.0000	-6.46
-.051270	2027	266.525	35.0000	-7.53
-.056152	2025	267.079	36.0000	-8.25
-.063477	2022	266.432	37.0000	-9.33

-.065918	2021	265.901	38.0000	-9.69
-.070801	2019	267.079	39.0000	-10.41
-.068359	2020	266.478	40.0000	-10.05
-.061035	2023	265.948	41.0000	-8.97
-.056152	2025	267.079	42.0000	-8.25
-.048828	2028	266.478	43.0000	-7.18
-.039063	2032	265.855	44.0000	-5.74
-.034180	2034	267.125	45.0000	-5.02
-.078125	2016	267.032	46.0000	-11.48
-.080566	2015	266.525	47.0000	-11.84
-.078125	2016	267.125	48.0000	-11.48
-.083008	2014	266.478	49.0000	-12.20
-.080566	2015	266.525	50.0000	-11.84
-.090332	2011	266.571	51.0000	-13.28
-.075684	2017	267.079	52.0000	-11.12
.427246	2223	267.079	53.0000	62.79
.266113	2157	266.432	54.0000	39.11
-.051270	2027	265.948	55.0000	-7.53
-.075684	2017	267.702	56.0000	-11.12
-.080566	2015	267.125	57.0000	-11.84
-.065918	2021	267.655	58.0000	-9.69
-.102539	2006	267.125	59.0000	-15.07
-.104980	2005	267.655	60.0000	-15.43
-.092773	2010	267.655	61.0000	-13.63
.236816	2145	267.748	62.0000	34.80
.551758	2274	267.655	63.0000	81.09
.031738	2061	268.302	64.0000	4.66
-.068359	2020	267.655	65.0000	-10.05
-.075684	2017	267.748	66.0000	-11.12
-.073242	2018	268.348	67.0000	-10.76
-.061035	2023	268.302	68.0000	-8.97
-.041504	2031	268.256	69.0000	-6.10
-.065918	2021	267.817	70.0000	-9.69
-.065918	2021	268.256	71.0000	-9.69
-.070801	2019	268.856	72.0000	-10.41
-.073242	2018	268.256	73.0000	-10.76
.073242	2078	268.256	74.0000	10.76
.551758	2274	268.256	75.0000	81.09
.163574	2115	268.302	76.0000	24.04
-.009766	2044	268.417	77.0000	-1.44
-.053711	2026	267.702	78.0000	-7.89
-.063477	2022	268.256	79.0000	-9.33
-.070801	2019	268.856	80.0000	-10.41
-.065918	2021	268.256	81.0000	-9.69
-.046387	2029	268.809	82.0000	-6.82
-.068359	2020	268.256	83.0000	-10.05
-.073242	2018	268.856	84.0000	-10.76
-.073242	2018	268.256	85.0000	-10.76
-.073242	2018	268.302	86.0000	-10.76

-.073242	2018	268.256	87.0000	-10.76
-.087891	2012	268.902	88.0000	-12.92
-.078125	2016	268.256	89.0000	-11.48
.007324	2051	269.433	90.0000	1.08
.495605	2251	268.902	91.0000	72.84
.212402	2135	268.856	92.0000	31.22
-.041504	2031	268.856	93.0000	-6.10
-.068359	2020	269.479	94.0000	-10.05
-.058594	2024	268.809	95.0000	-8.61
-.053711	2026	268.902	96.0000	-7.89
.270996	2159	269.433	97.0000	39.83
-.043945	2030	269.479	98.0000	-6.46
-.056152	2025	268.856	99.0000	-8.25
-.046387	2029	269.479	100.0000	-6.82
-.048828	2028	268.856	101.0000	-7.18
-.012207	2043	270.033	102.0000	-1.79
.217285	2137	268.256	103.0000	31.93
-.043945	2030	268.948	104.0000	-6.46
-.034180	2034	268.856	105.0000	-5.02
-.061035	2023	269.479	106.0000	-8.97
-.070801	2019	269.479	107.0000	-10.41
.144043	2107	270.079	108.0000	21.17
-.051270	2027	269.525	109.0000	-7.53
-.065918	2021	269.433	110.0000	-9.69
-.065918	2021	269.433	111.0000	-9.69
.068359	2076	268.417	112.0000	10.05
-.061035	2023	269.479	113.0000	-8.97
-.075684	2017	269.433	114.0000	-11.12
-.065918	2021	269.594	115.0000	-9.69
-.087891	2012	270.033	116.0000	-12.92
-.104980	2005	268.809	117.0000	-15.43
-.109863	2003	269.433	118.0000	-16.15
-.048828	2028	271.302	119.0000	-7.18
.083008	2082	269.640	120.0000	12.20
-.092773	2010	269.433	121.0000	-13.63
-.100098	2007	270.610	122.0000	-14.71
-.095215	2009	271.163	123.0000	-13.99
-.114746	2001	269.433	124.0000	-16.86
-.100098	2007	270.702	125.0000	-14.71
-.104980	2005	270.610	126.0000	-15.43
-.087891	2012	269.525	127.0000	-12.92
.048828	2068	270.079	128.0000	7.18
.109863	2093	270.610	129.0000	16.15
-.051270	2027	270.610	130.0000	-7.53
-.080566	2015	270.125	131.0000	-11.84
-.046387	2029	270.656	132.0000	-6.82
-.053711	2026	270.079	133.0000	-7.89
-.051270	2027	270.610	134.0000	-7.53
.048828	2068	270.817	135.0000	7.18

.031738	2061	269.525	136.0000	4.66
.180664	2122	270.610	137.0000	26.55
.119629	2097	270.610	138.0000	17.58
-.019531	2040	271.210	139.0000	-2.87
-.051270	2027	269.986	140.0000	-7.53
-.046387	2029	270.610	141.0000	-6.82
-.036621	2033	270.656	142.0000	-5.38
-.078125	2016	270.033	143.0000	-11.48
-.065918	2021	271.163	144.0000	-9.69
-.078125	2016	271.902	145.0000	-11.48
.056152	2071	270.610	146.0000	8.25
-.078125	2016	271.302	147.0000	-11.48
.178223	2121	271.210	148.0000	26.19
-.056152	2025	271.810	149.0000	-8.25
.222168	2139	271.210	150.0000	32.65
-.085449	2013	271.971	151.0000	-12.56
-.024414	2038	271.256	152.0000	-3.59
.031738	2061	270.610	153.0000	4.66
-.007324	2045	271.210	154.0000	-1.08
.253906	2152	271.256	155.0000	37.32
.102539	2090	271.810	156.0000	15.07
.263672	2156	271.163	157.0000	38.75
.261230	2155	270.033	158.0000	38.39
.163574	2115	271.256	159.0000	24.04
.058594	2072	271.163	160.0000	8.61
-.034180	2034	271.163	161.0000	-5.02
-.031738	2035	271.764	162.0000	-4.66
-.026855	2037	271.856	163.0000	-3.95
-.009766	2044	272.387	164.0000	-1.44
-.068359	2020	271.210	165.0000	-10.05
-.068359	2020	272.387	166.0000	-10.05
-.061035	2023	271.764	167.0000	-8.97
-.085449	2013	271.856	168.0000	-12.56
-.068359	2020	271.856	169.0000	-10.05
-.021973	2039	271.256	170.0000	-3.23
.175781	2120	271.810	171.0000	25.83
-.039063	2032	272.433	172.0000	-5.74
-.041504	2031	272.987	173.0000	-6.10
.046387	2067	272.387	174.0000	6.82
.156250	2112	272.479	175.0000	22.96
-.073242	2018	271.256	176.0000	-10.76
.036621	2063	271.856	177.0000	5.38
-.090332	2011	271.810	178.0000	-13.28
-.068359	2020	271.856	179.0000	-10.05
-.090332	2011	272.341	180.0000	-13.28
-.043945	2030	271.810	181.0000	-6.46
-.009766	2044	273.610	182.0000	-1.44
.048828	2068	271.810	183.0000	7.18
-.056152	2025	272.387	184.0000	-8.25

.058594	2072	273.033	185.0000	8.61
-.083008	2014	273.148	186.0000	-12.20
-.036621	2033	272.341	187.0000	-5.38
-.090332	2011	273.148	188.0000	-13.28
.224609	2140	272.387	189.0000	33.01
-.092773	2010	272.987	190.0000	-13.63
-.053711	2026	272.387	191.0000	-7.89
.305176	2173	273.564	192.0000	44.85
-.058594	2024	273.564	193.0000	-8.61
.031738	2061	273.564	194.0000	4.66
-.078125	2016	273.610	195.0000	-11.48
.256348	2153	271.856	196.0000	37.67
-.058594	2024	272.941	197.0000	-8.61
-.083008	2014	272.987	198.0000	-12.20
-.087891	2012	272.987	199.0000	-12.92
.263672	2156	272.941	200.0000	38.75

Appendix E

AVL 3057-A01 CHARGE AMPLIFIER
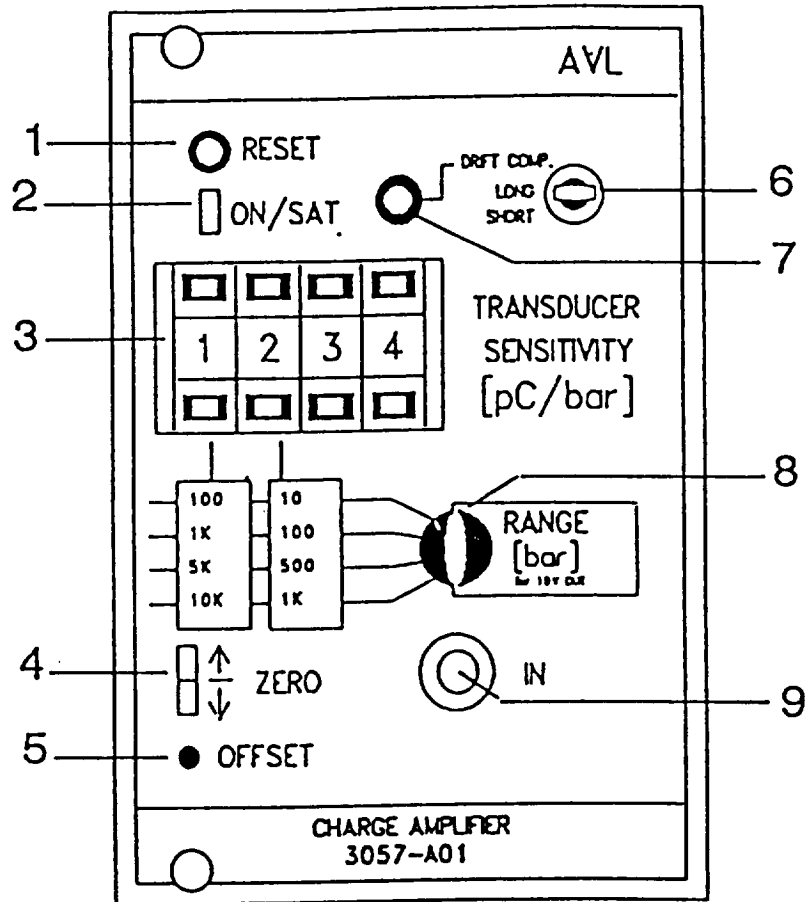
1) **RESET:**

Push button for discharging feedback capacitor.

2) **ON/SAT (2 functions):**

a) Power supply check light. Illuminated during operation

b) Saturation indicator: flashes when amplifier is driven into saturation.

3) **TRANSDUCER SENSITIVITY:**

Four-digit digital potentiometer for input of transducer sensitivity in pC/bar.

4) **ZERO:**

Indicates any deviation of the zero point from the quiescent potential in positive or negative direction.

5) **OFFSET**

Setting zero when RESET button is pressed. Check: neither ZERO LED is illuminated.

6) **LONG/SHORT/DRIFT COMP.:**

Operational mode selector switch

LONG :quasi-static measurement

SHORT :dynamic measurement

7) **DRIFT COMP. LED**

Not applicable.

8) **RANGE:**

Measuring range selector: 4-level decadic setting of measuring range; depending on decimal point of the measurement transducer sensitivity, one of the two columns will apply showing relevant input pressure for 10V output voltage.

9) **IN**

High insulation signal input connector socket for connecting pressure transducer with special high insulation, low noise cable.

CALIBRATION OF PRESSURE TRANSDUCER

Two options for calibrating the pressure transducer exist:
  A. Calibration by means of a dead weight tester (not discussed)[*]
  B. Manipulation of charge amplifier

MANIPULATION OF CHARGE AMPLIFIER:

This method is possible if the highest pressure expected during measurement, p_{max}, is known. To maintain a specific output voltage for a specific input pressure, an "incorrect" transducer sensitivity value can be set at the push button potentiometer. This value is derived from the following equation:

$$S = \frac{TRANS. \ SENS. \ x \ p_{max} \ measurement \ x \ V_{out} \ max(V)}{RANGE \ x \ V_{out} \ (V)}$$

  where: (S) is the value in pC/bar to be set at the potentiometer.
        V_{out} max always = 10V.
        TRANS. SENS. is in (pC/bar)
        p_{max} measurement is in (bar)
        RANGE is in (bar)

EXAMPLE: TRANS. SENS. : 2.23 pC/bar
        p_{max}:   600 bar
        V_{out}:   10 V

RANGE = 1 k. Derived from the position of the decimal point for the transducer sensitivity and p_{max} measurement

$$S = \frac{2.230 \ x \ 600 \ x \ 10}{1000 \ x \ 10} = 1.338$$

Setting the "incorrect" TRANS. SENS. at 1.338 pC/bar will give an output voltage of 10 V at a pressure of 600 bar
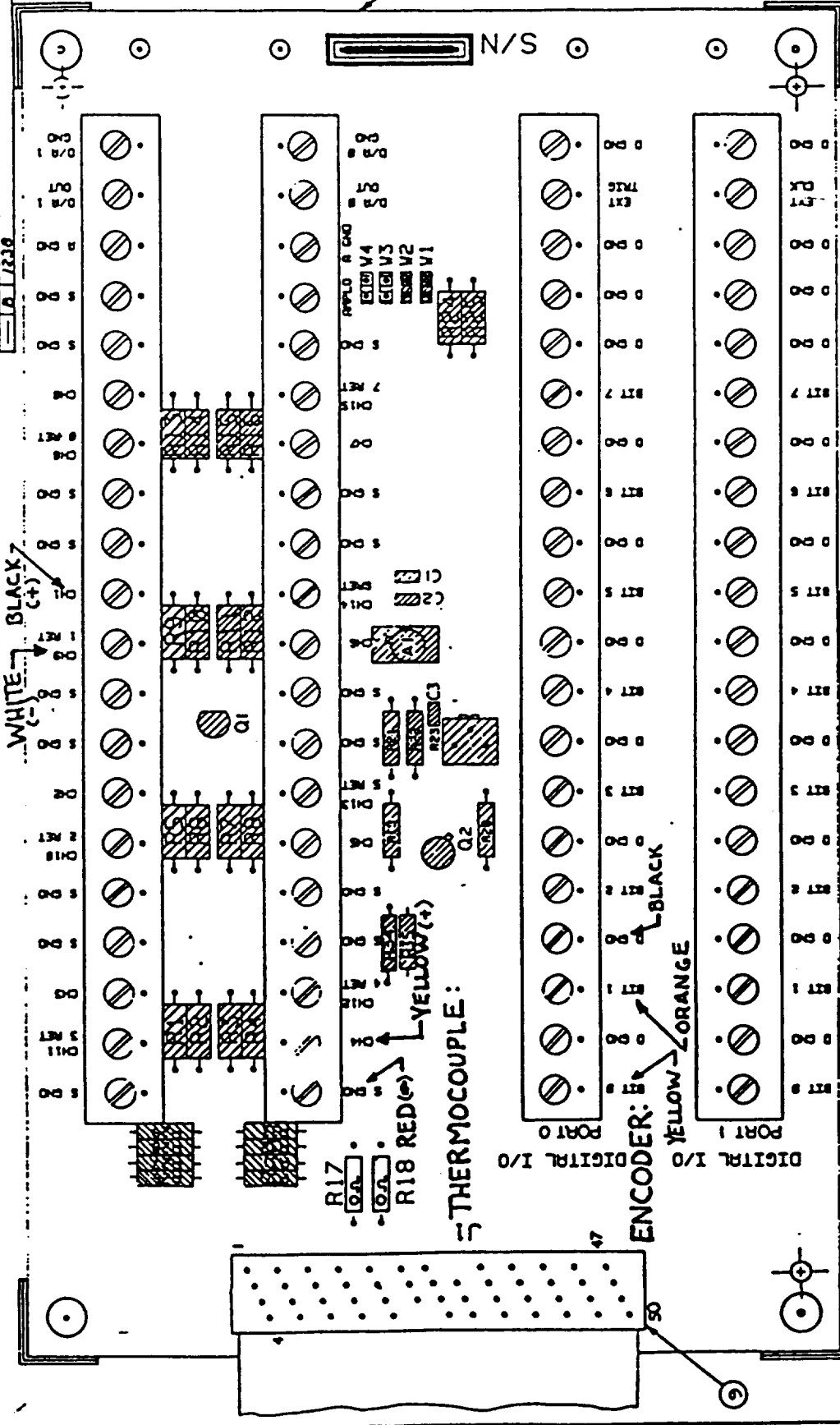
[*] This method is more accurate

NOTE:
HARDWARE
BOARD IS
MOUNTED
UPSIDE-DOWN
ON COMPUTER
STAND.

N/S

CHARGE AMPLIFIER FOR
PRESSURE TRANSDUCER:

WHITE (-)
BLACK (+)

THERMOCOUPLE:
R17
R18 RED (-)
YELLOW (+)

ENCODER:
YELLOW
ORANGE
BLACK

DIGITAL I/O
PORT 0
PORT 1

NOTES:
1. R22 TO BE MATCHED TO Q1
2. FOR LIST OF MATERIALS SEE A SIZE DWG GJ813

REF DES	DESCRIPTION
A1	OP21GP
C1,C2,C3	.1UF
R2,R3,R6,R7,R10,R11,R14,R15,R21	10K
R19	169K
R20	10.7K
R22	TRIM
R23	500Ω
R24	4K.0X%
R25	1K.02%
R35	100MEG
R26 THRU R33	12K
Q1	2N5086
Q2	LH0070-0H
	JUMPER PINS

707-T (PLUS THE FOLLOWING)

REF DES	DESCRIPTION
R34	2.2K

707

REF DES	DESCRIPTION
J1	BARRIER STRIP
	CABLE ASSY
R17,R18	0Ω
W3,W1	JUMPER PINS

707-M

REF DES	DESCRIPTION
J1	BARRIER STRIP
	CABLE ASSY
R17,R18	0Ω
W3,W4	JUMPER PINS
R1,R4,R5,R8,R9,R12,R13,R16	250Ω-.05%
R2,R3,R6,R7,R10,R11,R14,R15	10K

Ø	ENGINEERING PROTOTYPE			
1	REVISED			
A	RELEASED FOR PRODUCTION			

C | SEE ECO 1315
D | ECO 1728

DATA TRANSLATION

COMPONENT BOARD ASSEMBLY
DT707 (TABULATED)

C | 00817

DT 707

```
*          PROGRAMMER:  SCOTT A. HOOVER
*                DATE:  SPRING 1993
*              COURSE:  MEM434/SENIOR DESIGN PROJECT
*             ADVISOR:  DR. C.P. BRITCHER
*
*          'TEAM Med':  MARS ENGINE DESIGN
*
*
           PROGRAM MARS
*
*
*          configuration functions:
           INTEGER*2 LPINIT,LPSB,LPST,LPTERM
*
*          analog input functions:
           INTEGER*2 LPAV,LPAOT,LPSETA,LPADS,LPBAD,LPCAD,LPTAD,LPWAD,LPSAD
*          analog output functions:
           INTEGER*2 LPDV,LPSETD,LPDAS,LPBDA,LPCDA,LPTDA,LPWDA,LPSDA
*          digital I/O functions:
           INTEGER*2 LPEFO,LPEFI,LPODV,LPIDV
*          clock functions:
           INTEGER*2 LPRCF,LPSCF,LPDSC,LPESC
*          data manipulations:
           INTEGER*2 LPMV,LPGV,LPMT,LPMC,LPVTD,LPDTV,LPATV,LPVTA
*          error processor functions;
           INTEGER*2 LPSECW,LPGEC
*
           INTEGER*2 STATUS,TC,CHAN
           INTEGER*2 STRTCHN,ENDCHN,GAIN
           INTEGER*2 COUNT,TIMING,ARRAY(1000)
           INTEGER*2 PORT,MASK,VALUE,ARAY(1000)
           REAL*4 FREQ,TIME,PRESS
           REAL*4 DEG,VOLTS
*
*          lpclab subroutines - fortran definition files
*
           OPEN(UNIT=13,FILE='DATA.O',STATUS='OLD')
           TIMING = 0
           STRTCHN = 1
           ENDCHN = 1
           GAIN = 1
           TIME = 0
           PRESS = 0
           PRINT*,'INPUT THE FREQUENCY FOR THIS RUN:'
           READ*, FREQ
           PRINT*,'INPUT THE NUMBER OF COUNTS'
           READ*, COUNT
           PRINT*,'INPUT THE NUMBER OF (D/A) VALUES TO BE READ FROM ENCODER'
           READ*, VALUE
*
           CHAN= 4
           TC=75
           PORT = 0
           MASK = 11
*
           STATUS = LPINIT()
           STATUS = LPSB(1)
           STATUS = LPST(0)
           STATUS = LPSCF(FREQ)
           STATUS = LPSETA(TIMING,STRTCHN,ENDCHN,GAIN)
```

```
       STATUS = LPBAD(COUNT,ARRAY(1))
       STATUS = LPWAD(ARRAY(COUNT))
       STATUS = LPMT(TC,CHAN,DEG)
*
*      ************************************************************
*      *            THERMOCOUPLE TEMPERATURE FOR EXHAUST          *
*      ************************************************************
       PRINT 5
  5    FORMAT(1X,'TEMPERATURE OF THE THERMOCOUPLE (CELCIUS)')
       PRINT*,DEG
       WRITE(13,10)
  10   FORMAT(1X,'THERMOCOUPLE TYPE',3X,'CHANNEL',3X,'TEMPERATURE (C)')
       WRITE(13,*)TC,CHAN,DEG
       WRITE(13,15)
  15   FORMAT(1X,'THE FREQUENCY OF THIS RUN IS:')
       WRITE(13,*)FREQ
       WRITE(13,*)
       WRITE(13,20)
  20   FORMAT(1X,'THE NUMBER OF COUNTS:')
       WRITE(13,*) COUNT
*
*      ************************************************************
*      *            PRESSURE FOR AVL PRESSURE TRANSDUCER          *
*      ************************************************************
       WRITE(13,*)
       WRITE(13,*)
       WRITE(13,25)
  25   FORMAT(5X,'VOLTS',10X,'DIGITAL VALUE',5X,'TIME(SEC)',10X,
      +'PRESSURE(PSIG)')
       DO 100 I=1,COUNT
       STATUS = LPATV(ARRAY(I),GAIN,VOLTS)
       PRESS=(VOLTS*10*1.0133E5)/6894.76
       TIME=TIME + (1/FREQ)
       WRITE(13,30)VOLTS,ARRAY(I),TIME,PRESS
  30·  FORMAT(1X,E12.6,10X,I5,10X,F7.5,14X,F6.2)
  100  CONTINUE
*
*      ************************************************************
*      *                 ENCODER ANGLE PROGRAM                    *
*      ************************************************************
       WRITE(13,*)
       WRITE(13,*)
       WRITE(13,35)
  35   FORMAT(5X,'DIGITAL VALUE',5X,'ENCODER ANGLE')
       DO 200 I=1,VALUE
       STATUS = LPIDV(PORT,MASK,ARAY(I))
*       PRINT*,ARAY(I)
*       WRITE(13,40)ARAY(I)
  40   FORMAT(1X,I3)
  200  CONTINUE
       END
```